Effects of an oscillating magnetic field on homogeneous ferrofluid turbulence

Kristopher R. Schumacher*
Department of Chemical Engineering, University of Washington, Seattle, Washington 98195, USA

James J. Riley
Department of Mechanical Engineering, University of Washington, Seattle, Washington 98195, USA

Bruce A. Finlayson†
Department of Chemical Engineering, University of Washington, Seattle, Washington 98195, USA

(Received 14 October 2009; published 26 January 2010)

This paper presents the results from direct numerical simulations of homogeneous ferrofluid turbulence with a spatially uniform, applied oscillating magnetic field. Due to the strong coupling that exists between the magnetic field and the ferrofluid, we find that the oscillating field can affect the characteristics of the turbulent flow. The magnetic field does work on the turbulent flow and typically leads to an increased rate of energy loss via two dissipation modes specific to ferrofluids. However, under certain conditions this magnetic work results in injection, or a forcing, of turbulent kinetic energy into the flow. For the cases considered here, there is no mean shear and the mean components of velocity, vorticity, and particle spin rate are all zero. Thus, the effects shown are entirely due to the interactions between the turbulent fluctuations of the ferrofluid and the magnetic field. In addition to the effects of the oscillation frequency, we also investigate the effects of the choice of magnetization equation. The calculations focus on the approximate centerline conditions of the relatively low Reynolds number turbulent ferrofluid pipe flow experiments described previously [K. R. Schumacher *et al.*, Phys. Rev. E **67**, 026308 (2003)].

DOI: 10.1103/PhysRevE.81.016317 PACS number(s): 47.65.Cb, 47.27.Gs, 47.27.ek

I. INTRODUCTION

Ferrofluids are stable colloidal suspensions of nanoscale ferromagnetic particles that exhibit strong responses to applied magnetic fields. For example, a steady magnetic field applied to a shear flow hinders the free-rotation of the suspended particles, and results in an increase in effective viscosity [1] due to an additional rotational frictional resistance. This frictional resistance is also exhibited when a steady magnetic field is applied to homogenous ferrofluid turbulence, which has no mean shear [2]. A time-dependent magnetic field has this same effect at low oscillation frequencies, but, under special conditions, the field can cause the suspended particles to rotate faster than the local fluid rotation rate [3]. This phenomena, which has been shown experimentally for laminar shear flows, results in a decrease in the effective viscosity relative to its zero-field value [4,5]. Turbulent ferrofluid pipe flow experiments [6] examined the effects of an oscillating magnetic field on the pressure drop at different flow rates, magnetic field strengths, and oscillation frequencies. However, the effects of oscillating magnetic fields on ferrofluid flows in the turbulent regime are not fully understood. In this paper, the effects of an oscillating magnetic field on the characteristics of a homogeneous turbulent ferrofluid flow are examined using direct numerical simulation (DNS) of the governing equations of ferrohydrodynamics. The equations for turbulent ferrofluid flows are described more fully in Schumacher *et al.* [2].

Homogeneous turbulent flow is studied with an unidirectionally applied magnetic field, in the present case in the x direction, that oscillates in time. The applied oscillating magnetic fields considered here are characterized by $H_x = H_{o_x} \cos(\Omega t)$, where H_{o_x} is the amplitude and Ω is the oscillation frequency. One of the unique features of ferrofluids is that particles can be made to spin somewhat independently of the flow so that their angular velocity is not necessarily one-half the vorticity. First, the effect of the three magnetization equations are studied. Then one of those magnetization equations is used for a variety of magnetic field amplitudes, frequency of oscillation, and magnetic time constants τ_B. The results are compared with, and sometimes bounded by, those for a Newtonian fluid and a ferrofluid with a large, steady magnetic field. Finally, we examine the effects of an oscillating field under the same conditions as the pipe flow experiments in [6].

Bacri *et al.* [4] studied the effects of $\Omega\tau_B$ when an oscillating magnetic field is applied to laminar ferrofluid Poiseuille pipe flow with an axial magnetic field that oscillates in time. Their theoretical and experimental work showed that the effective viscosity is increased for slow oscillations but is decreased for faster oscillations. The ratio $\mu_{\text{eff}}/\mu > 1$ when $\Omega\tau_B < 1$, and $\mu_{\text{eff}}/\mu < 1$ when $\Omega\tau_B \sim 1$, where μ_{eff} is the measured effective viscosity of the fluid, μ is the viscosity of the ferrofluid when the magnetic field is turned off, and τ_B is the Brownian particle relaxation time. When $\Omega\tau_B < 1$, the period of the oscillating magnetic field is bigger than τ_B, the magnetic field changes slowly, and the magnetic field hinders particle rotation: the rotation rate of the particles is less than that of the surrounding fluid. The additional friction within the substructure of the fluid caused by the fluid having to

*Present address: 18000 East 29th Terrace Court South, Independence, MO 64057.
†Corresponding author. finlayso@u.washington.edu

flow around the particles shows up macroscopically as an increased viscosity. When $\Omega\tau_B > 1$, the period of the oscillating magnetic field is smaller than τ_B. Then, the time-average of the torque term in the spin equation is positive and the net effect is to rotate the particles faster than the surrounding fluid. This injects energy into the flow and shows up macroscopically as a reduced viscosity. The pipe flow system of Bacri *et al.* [4] had a mean shear in laminar flow, but we examine the same phenomena in homogeneous turbulent flow with zero mean shear.

II. EQUATIONS AND NUMERICAL METHOD

A. Governing equations

Dynamic ferrofluid flows are well described by the equations of ferrohydrodynamics [7]. The continuity and momentum equations are

$$\nabla \cdot \mathbf{u} = 0, \tag{1}$$

$$\rho\left(\frac{\partial \mathbf{u}}{\partial t} + \mathbf{u}\cdot\nabla\mathbf{u}\right) = -\nabla p + 2\mu\,\nabla\cdot\mathbf{e} + \zeta\,\nabla\times(2\boldsymbol{\omega} - \nabla\times\mathbf{u}) + \mu_o\mathbf{M}\cdot\nabla\mathbf{H}, \tag{2}$$

where ρ is the density, μ is the viscosity, ζ is the vortex viscosity, μ_o is the permeability of free space, $\mathbf{u}$ is the velocity, p is the pressure, $\boldsymbol{\omega}$ is the spin, $\mathbf{e}=0.5(\nabla\mathbf{u}+\nabla\mathbf{u}^T)$ is the rate of strain tensor, $\mathbf{M}$ is the magnetization vector, and $\mathbf{H}$ is the applied magnetic field. The internal angular momentum equation (i.e., spin equation) is

$$\rho I\left(\frac{\partial \boldsymbol{\omega}}{\partial t} + \mathbf{u}\cdot\nabla\boldsymbol{\omega}\right) = 2\eta'\,\nabla\cdot\mathbf{s} + 2\zeta(\nabla\times\mathbf{u} - 2\boldsymbol{\omega}) + \mu_o\mathbf{M}\times\mathbf{H}, \tag{3}$$

where I is the moment of inertia of a single ferrofluid particle, η' is the spin viscosity, and $\mathbf{s}=0.5(\nabla\boldsymbol{\omega}+\nabla\boldsymbol{\omega}^T)$ is the spin-rate gradient tensor. The spin equation can be simplified to give

$$\boldsymbol{\omega} = \frac{1}{2}\nabla\times\mathbf{u} + \frac{\mu_o}{4\zeta}\mathbf{M}\times\mathbf{H} \tag{4}$$

since the moment of inertia of the ferrofluid particles is so small and the spin viscosity term leads to negligible effects [2]. Note that the magnetic torque influences $(\nabla\times\mathbf{u}-2\boldsymbol{\omega})$, which then provides a new force in the momentum equation.

A magnetization equation is necessary to form a closed set of equations. Different magnetization equations have been proposed in the literature (e.g., [8–10]). Most simulations described here employ the Martsenyuk *et al.* [9] equation, which is based on the Fokker-Planck equation using the effective field method for dilute ferrofluids. The Martsenyuk, *et al.* equation is

$$\frac{\partial \mathbf{M}}{\partial t} = -\mathbf{u}\cdot\nabla\mathbf{M} + \left(\frac{1}{2}\nabla\times\mathbf{u}\right)\times\mathbf{M} - \frac{3\chi_o}{2\tau_B M^2}\left(1 - \frac{3L(\xi_e)}{\xi_e}\right)\mathbf{M}\times(\mathbf{M}\times\mathbf{H}) - \frac{1}{\tau_B}\left[\mathbf{M} - \frac{3\chi_o L(\xi_e)}{\xi_e}\mathbf{H}\right], \tag{5}$$

where $\chi_o=\lim_{H\to 0}(M_0/H)=(\mu_o m M_S)/(3k_BT)$ is the initial magnetic susceptibility, τ is the magnetic particle relaxation time, which is taken to be the same as τ_B here. The parameter ξ_{ei} is the nondimensional effective magnetic field for which the nonequilibrium magnetization, M_i, is an equilibrium magnetization. The effective field is related to M_i by the equation

$$M_i = M_S L(\xi_e)\frac{\xi_{ei}}{\xi_e},$$

where

$$\xi_{ei} = \frac{\mu_o m H_{ei}}{k_B T} \quad \text{and} \quad L(\xi) = \frac{1}{\tanh(\xi)} - \frac{1}{\xi}.$$

Here, m is the magnetic moment of a single particle, k_B is Boltzmann's constant, T is the absolute temperature, and M_s is the saturation magnetization.

Section III A utilizes two other versions of the magnetization equation: the Shliomis [8] equation and the Felderhof and Kroh [10] equation. The Shliomis equation [8] is given as

$$\frac{\partial \mathbf{M}}{\partial t} = -\mathbf{u}\cdot\nabla\mathbf{M} + \boldsymbol{\omega}\times\mathbf{M} - \frac{1}{\tau}(\mathbf{M} - \mathbf{M}_0), \tag{6}$$

where $\mathbf{M}_0=M_S L(\xi)H/H$ and $H=\sqrt{H_x^2+H_y^2+H_z^2}$. The Felderhof and Kroh equation [10], which is based on irreversible thermodynamics, is

$$\frac{\partial \mathbf{M}}{\partial t} = -\mathbf{u}\cdot\nabla\mathbf{M} + \boldsymbol{\omega}\times\mathbf{M} - \frac{\chi_o}{\tau}[\mathbf{H} - \mathbf{H}_{\mathrm{eq}}], \tag{7}$$

where $\mathbf{H}_{\mathrm{eq}}$ is the local equilibrium magnetic field.

Finally, to complete the set of equations, Maxwell's equations are

$$\nabla\cdot\mathbf{B} = 0, \tag{8}$$

$$\nabla\times\mathbf{H} = 0. \tag{9}$$

Note that the magnetization is related to $\mathbf{B}$ and $\mathbf{H}$ via $\mathbf{B} \equiv \mu_0(\mathbf{M}+\mathbf{H})$.

B. Energetics

The total turbulent kinetic energy in a ferrofluid flow consists of a translational component, $E_t=\frac{1}{2}\rho\overline{u_i'^2}$, and a rotational component, $E_r=\frac{1}{2}\rho I\overline{\omega_i'^2}$, where the prime denotes a fluctuating quantity. The general transport equations for E_t and E_r can be derived from the momentum and internal angular momentum equations, respectively [2]. For the specific case of

TABLE I. Ferrofluid (EMG-206) parameters (same as in Ref. [2]).

Physical parameter	Value
T (K)	298.15
μ (Pa s)	3.85×10^{-3}
ρ (kg m^{-3})	1187.4
m (A m^2)	2.5×10^{-19}
M_s (Oe)	164
τ (μs)	10
ζ (Pa s)	0.55μ
I (m^2)	7.57×10^{-17}
η' (kg m s^{-1})	2×10^{-15}
χ_o	0.332

TABLE II. Time averaged flow properties of the initial ferrofluid velocity field (same as in Ref. [2]).

Flow property	Value
$u_{\rm rms}$ (cm s^{-1})	20.63
$\mathcal{L}$ (cm)	0.1
$\mathcal{T}$ (s)	0.00485
Re_λ	37.3
λ (cm)	0.0586
η (cm)	0.00487
τ_η (s)	7.324×10^{-4}
$k_{\max}\eta$	2.0

homogeneous turbulence, the turbulent energy equations are reduced, by ignoring spatial gradients of all averaged quantities, to give

$$\frac{dE_t}{dt} = -\varepsilon - \varepsilon_A - \Phi^b + \Psi, \tag{10}$$

$$\frac{dE_r}{dt} = -\varepsilon_C + \Phi^b + \Psi_s, \tag{11}$$

$$\frac{dU}{dt} = \varepsilon + \varepsilon_A + \varepsilon_C. \tag{12}$$

Equation (12) represents the internal energy equation when there are no heat sources or fluxes. The terms on the right-hand side of Eqs. (10)–(12) represent different modes, or pathways, of energy transfer within the system. The term $\varepsilon=2\mu\overline{e'_{ij}e'_{ij}}$ is the classical rate of viscous dissipation of turbulent kinetic energy, $\varepsilon_A=\frac{1}{4\zeta}\overline{A'_iA'_i}$ is called the vortex viscous dissipation rate, where $A'_i=2\zeta(\varepsilon_{ikl}u'_{l,k}-2\omega'_i)$, and $\varepsilon_C=2\eta'\overline{s'_{ij}s'_{ij}}$ is the spin viscous dissipation rate. The term $\Phi^b=\overline{\omega'_iA'_i}$ represents the work rate done on the spin by asymmetric stresses, $\Psi=\overline{u'_iS'_i}$ is the work rate done on the turbulent flow by the magnetic body forces, where $S'_i=\mu_oM'_kH'_{i,k}$, and $\Psi_s=\overline{\omega'_iQ'_i}$ denotes the rate of work done by the magnetic body couple forces on the turbulent flow, and $Q'_i=\mu_o\varepsilon_{ikl}M'_kH'_l$. Each of these terms can be directly computed in our direct turbulence simulations. Thus, Eqs. (10)–(12) provide a useful framework for investigating how the applied oscillating magnetic fields affect the physics of the flow.

C. Fluid parameters

The ferrofluid we simulate is the water-based EMG-206, from Ferrotec, which is the same experimental fluid investigated in previous studies [2,6]. The fluid and magnetic properties of EMG-206 (determined and described previously [2,6]) are summarized here in Table I.

D. Numerics and initial velocity

We simulate statistically homogeneous turbulent ferrofluid flow in a cube with periodic boundary conditions. For the oscillating magnetic fields here, we expand the technique described in Schumacher *et al.* [2] for steady magnetic fields. The side length of the cube is L, which is large compared to the integral length scale of the flow $\mathcal{L}$. The variables are expanded using a finite Fourier series in each spatial dimension. For example, the velocity is expanded as

$$u(\mathbf{x}) = \sum_{k_x=-N/2}^{N/2}\sum_{k_y=-N/2}^{N/2}\sum_{k_z=-N/2}^{N/2}\hat{u}(\mathbf{k})e^{i\mathbf{k}\cdot\mathbf{x}}, \tag{13}$$

where the wavenumbers k_x, k_y, and k_z range from $-N/2$ to $N/2$. This Fourier expansion is done for each dependent variable. A pseudospectral method is employed to directly solve the governing equations. The derivatives are efficiently evaluated in Fourier space and the nonlinear terms are computed in physical space then transformed back to Fourier space and dealiased. The flow is forced by injecting energy into the low wavenumber range using the method described in Zikanov and Thess [11].

When the particle relaxation time is much smaller than the Kolmogorov scale and/or the magnetic field changes rapidly relative to the smallest scales of turbulence, i.e., $\Omega\tau_\eta \gg 1$, the equations are stiff. In addition, there are 45 required Fourier transforms per time step for a ferrofluid, as opposed to 9 for a Newtonian fluid. Thus, the computational cost is significantly larger than for a Newtonian fluid.

Before the magnetic field is turned on, the flow is allowed to develop to a statistically stationary state. The initial velocity field used here is the same as in the steady magnetic field simulations [2]. We set the energy in the forcing shell (i.e., where $k<2.5\ \mathrm{k_{min}}$) to equal 70% of the estimated centerline turbulent kinetic energy of a steady-state turbulent ferrofluid pipe flow at $\mathrm{Re}\sim3100$ [6]. The pipe in [6] has a 0.3 cm diameter and the turbulent kinetic energy distribution is estimated using a k-ε model. The properties of the flow before the magnetic field is turned on are summarized in Table II, where $u_{\rm rms}$ is the root-mean square velocity, $\mathcal{T}=\frac{\mathcal{L}}{u_{\rm rms}}$ is the large eddy turnover time, and $\mathcal{L}=\frac{\pi}{2u_{\rm rms}^2}\int_{k=0}^{\infty}\frac{E_t(k)}{k}dk$ is the integral length scale. The Taylor microscale Reynolds number is $\mathrm{Re}_\lambda=\lambda u_{\rm rms}/\nu$, where the Taylor microscale is $\lambda=\sqrt{10\nu E_t/\varepsilon}$. The Kolmogorov length and time scales are η and τ_η. Finally, Pope [12] discusses that the smallest scales of fluid

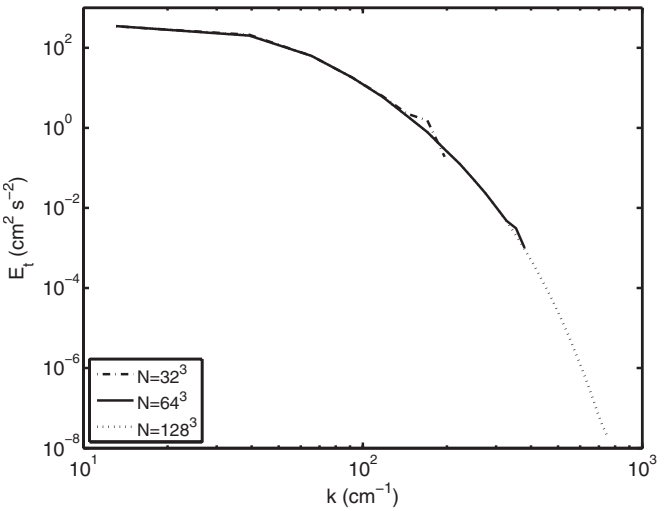

FIG. 1. Comparison of the spectrum of the turbulent kinetic energy when using 32^3, 64^3, and 128^3 modes when $H=316$ Oe and $\Omega=60$ Hz with the Shliomis (Ref. [8]) magnetization equation. The spectral comparison is shown at the end of 6.19 large eddy turnover times (T), where $T=0.00485$ s.

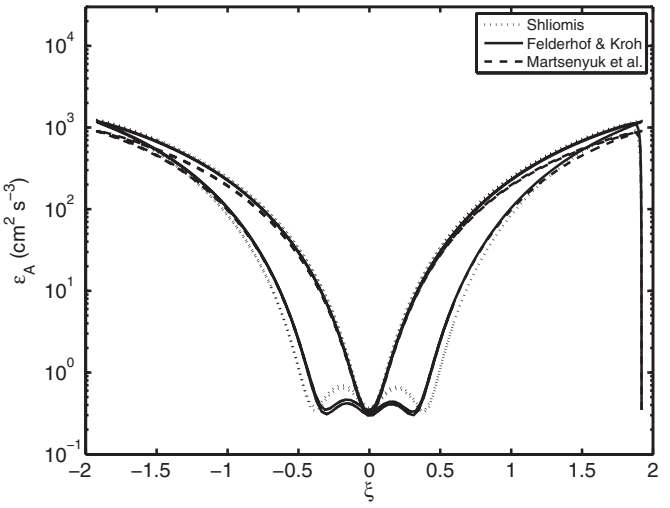

FIG. 2. Vortex viscous dissipation due to the antisymmetric part of the stress versus normalized applied magnetic field; $\xi=1.92$ ($H=316$ Oe) and $\Omega\tau_B=0.02\pi$. Magnetic equations of Shliomis (Ref. [8]), Felderhof and Kroh (Ref. [10]), and Martsenyuk *et al.* (Ref. [9]). As the magnetic field oscillations in time, ξ goes from −1.92 to +1.92.

motion are well resolved when $k_{\max}\eta \geq 1.5$; note that for our simulations $k_{\max}\eta=2.0$.

The value of Re_λ is low ($\sim$37) for the simulated cases. In view of the smaller time step and fivefold increase in the number of unknowns, we need to carefully choose the number of Fourier modes. Kerr [13] performed DNS calculations of homogeneous flows with a range of $\mathrm{Re}_\lambda=28-56$ using 64^3 modes, and this number of modes was adequate for full resolution of the flow. For comparison, Gotoh *et al.* [14] did simulations at $\mathrm{Re}_\lambda=460$ using 1024^3 modes, and Kaneda *et al.* [15] did simulations at $\mathrm{Re}_\lambda=1200$ using 4096^3 modes. The flows we are studying are at much smaller values of Re_λ, taking values from 36 to 38. Thus, simulations are feasible using the computational resources of a single desktop PC; we employ 64^3 modes in our simulations, and these are confirmed by a few calculations using 128^3 modes. The spectrum of the turbulent kinetic energy is shown in Fig. 1 for 32^3, 64^3, and 128^3 modes and the solutions with 64^3 modes show good agreement with those with 128^3 modes for wave numbers that overlap.

III. RESULTS

A. Effect of magnetization equation

In the homogeneous ferrofluid simulations of Schumacher *et al.* [2], the effects of the choice of magnetization equation were studied with a constant magnetic field and gave similar turbulence results at the smaller magnetic fields ($\xi<2$). In this section, we test whether the same is true for an oscillating field when $\xi=1.92$ and $\Omega\tau_B=0.02\pi$. Note that in the ferrofluid pipe flow experiments [6], the magnetic field magnitude ranges from 0 to 1264 Oe ($\xi=0-7.68$), and the oscillation frequency ranges from 0 to 1000 Hz ($\Omega\tau_B=0-0.02\pi$).

For these cases, standard homogeneous turbulence properties that depend on velocity and vorticity, e.g., the turbulence intensity and classical dissipation rates, are found to be not significantly affected by the choice of magnetization equation. This corresponds with the results of Schumacher *et al.* [2]. In ferrofluids, the internal angular momentum is more sensitive to the magnitude of the applied field than velocity or vorticity. Thus, to further check potential effects, we study the vortex viscous dissipation ε_A, which depends on the square of the antisymmetric part of the stress.

Figure 2 shows a limit cycle of ε_A as a function of normalized magnetic field strength for the first few cycles of the magnetic field. Although the results are similar for all magnetization equations, slight deviations are apparent. The deviations that occur in the $\bar{\xi}>1$ range are due to the magnitude of the magnetic field and not the oscillation frequency. When the magnetic field changes sign in the time cycle and the magnitude of ξ is still small ($\bar{\xi}<0.5$), the lines are not always superimposed. This is despite the fact that the torques are effectively the same when $\bar{\xi}<0.5$ in nonoscillating cases [2].

The ratio of magnetic particle relaxation time to period of oscillation in this case is small, and it has a minimal influence on the velocity, vorticity, and vortex viscous dissipation, ε_A, as was the case with a steady field [2]. Thus, the DNS results at the highest frequency used in the pipe flow experiment [6] are essentially independent of magnetization equation as long as $\xi<2$. In the following work when $\xi=7.68$(Figs. 2–11) we use the Martsenyuk *et al.* [9] magnetization equation, but use the Shliomis [8] equation when $\xi=1.92$(Fig. 12).

B. Effect of oscillation frequency

This section demonstrates the effect of the oscillation frequency when $\xi=7.68$ and compares with earlier results for a steady field [2]. The simulations here employ the Mart-

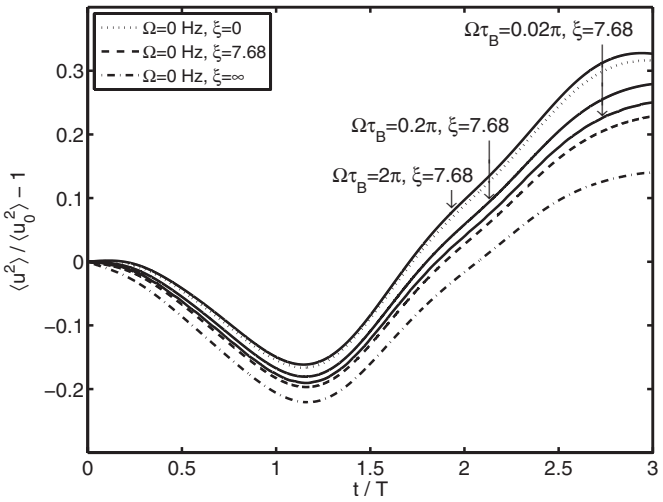

FIG. 3. Normalized mean square velocity vs normalized time. The mean square velocity, $\langle u^2 \rangle$, is normalized by the mean square velocity at $t=0$, $\langle u_0^2 \rangle$, and the time is normalized by the large eddy turnover time, T, where $T=0.00485$ s.

senyuk *et al.* [9] magnetization equation. In particular, changes in the root-mean-square velocity, Taylor microscale, and spin/vorticity differences are examined. The effect on effective viscosity and transfer of energy between modes is also described.

A key nondimensional parameter is $\Omega \tau_B$, which relates the relaxation time of the particle to the characteristic time of the oscillating magnetic field. In the simulations here the values of $\Omega \tau_B$ are $2\pi/100$, $2\pi/10$, and 2π, respectively ($\tau_B = 10$ μs). In all cases, the period of the magnetic field is fast compared to the Kolmogorov time of the turbulent flow; the values for the nondimensional product $\Omega \tau_\eta$ are 4.6, 46, and 460, respectively ($\tau_\eta = 7.324 \times 10^{-4}$ s). The extra number of discreet time steps required to resolve the magnetic field makes this a stiff problem.

In Schumacher *et al.* [2] for a steady magnetic field it was shown (p. 22) that the time-averaged terms coming from the magnetic body force and magnetic convection terms could

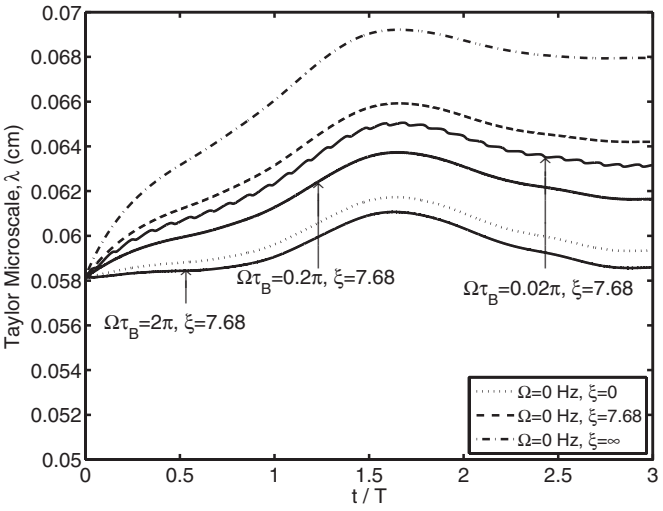

FIG. 4. Taylor microscale vs time normalized by the large eddy turnover time.

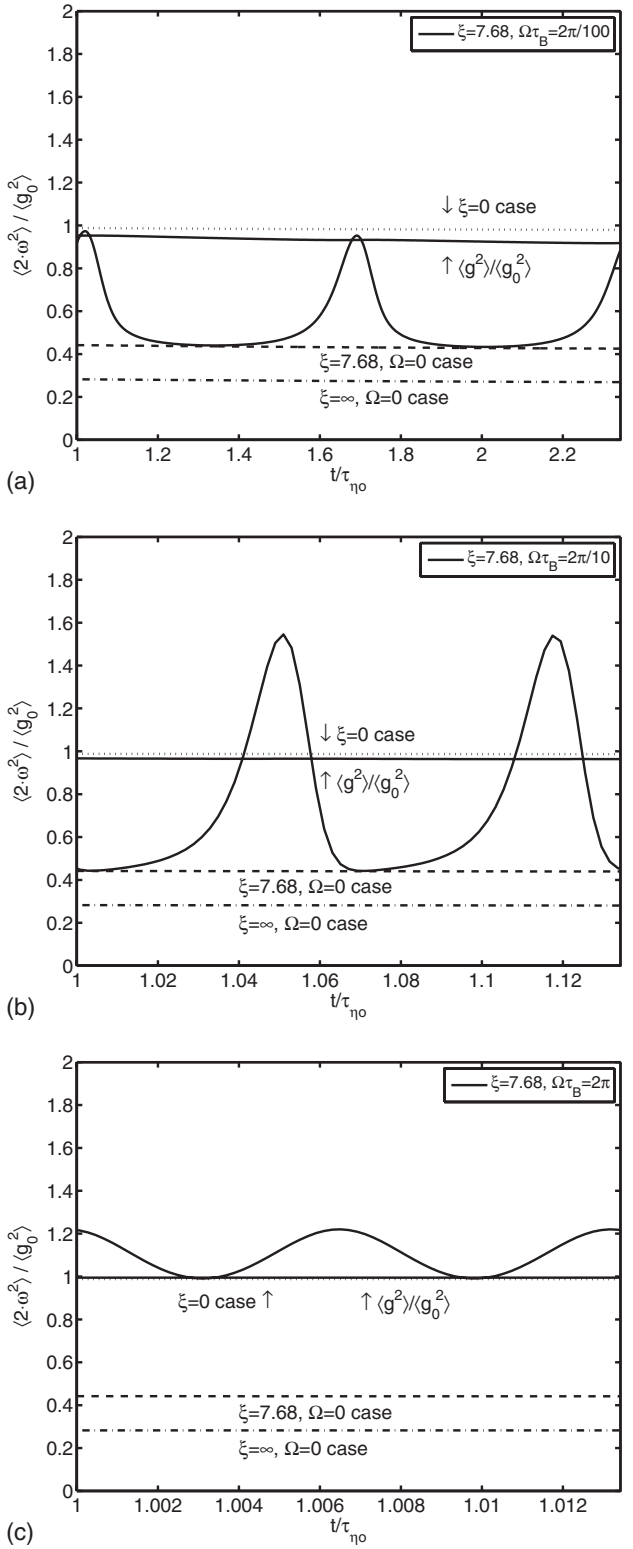

FIG. 5. Mean square spin and mean square vorticity vs time. All panels: dotted line—$\xi=0$, nonoscillating limit; dashed line—$\xi=7.68$, nonoscillating limit; dash-dot line—$\xi=\infty$ nonoscillating limit.

be ignored. The terms are the magnetic body force in the momentum equation, $\mu_o M_k H_{i,k}$, and the magnetic convection term, $u_k M_{i,k}$, in the magnetization equation. This hypothesis was tested for an oscillating magnetic field by solving the

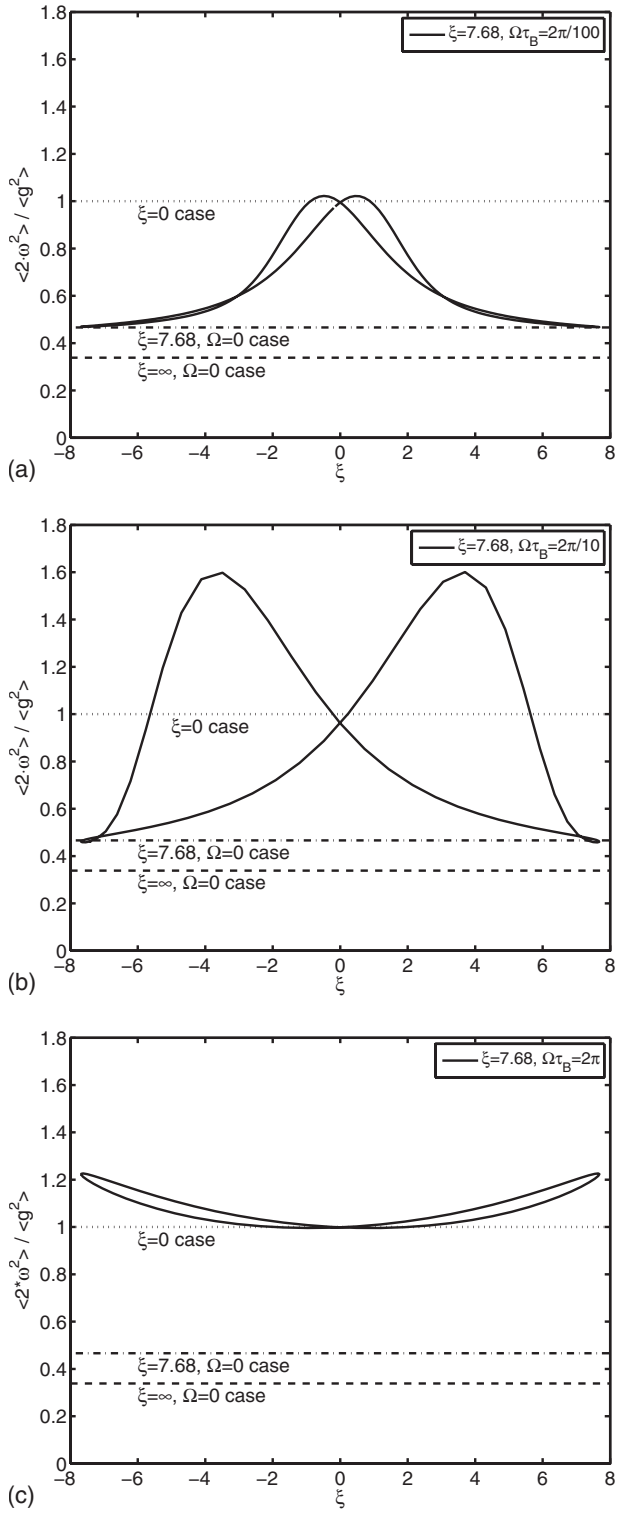

FIG. 6. Limit cycles of twice the mean square spin normalized by the mean square vorticity vs nondimensional magnetic field strength. All panels: dotted line—$\xi=0$, nonoscillating limit; dash-dot line—$\xi=7.68$, nonoscillating limit; dashed line—$\xi=\infty$ nonoscillating limit.

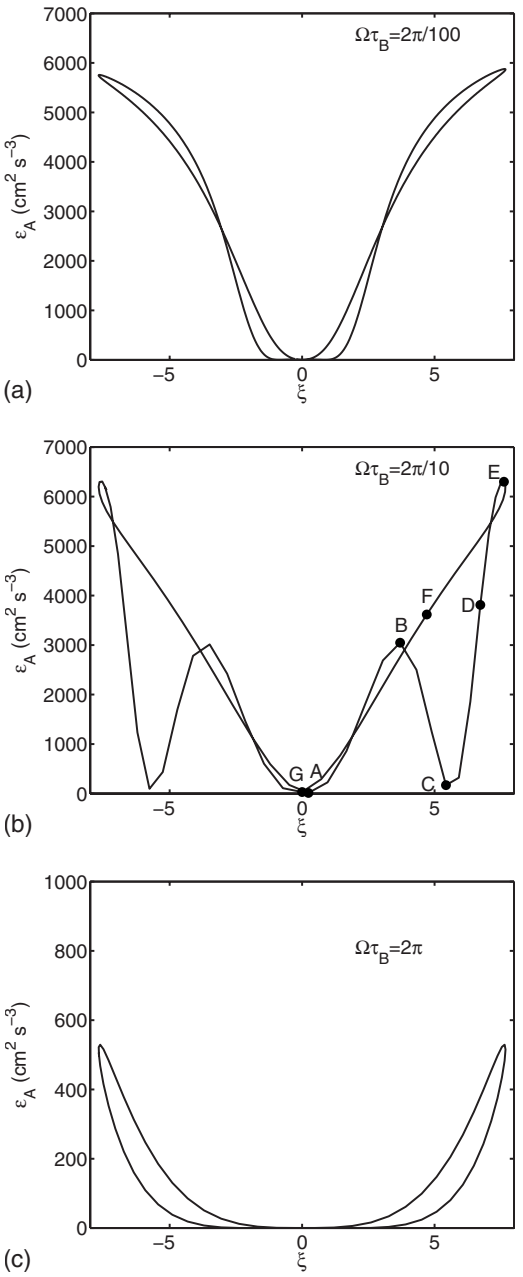

FIG. 7. Limit cycles of vortex viscous dissipation rate vs ξ. Magnetic field amplitude of $\xi=7.68$, and using the Martsenyuk (Ref. [9]) magnetization equation. Oscillation frequencies of (a) $\Omega\tau_B=2\pi/100$, (b)$2\pi/10$, and (c)2π. The labels (A–G) in panel (b) correspond to the spectra in Fig. 9.

problem both including and ignoring these terms for the case when they would be the biggest: $H=1264$ Oe and $\Omega=100$ kHz. The results for 64^3 and 128^3 modes without the terms are almost identical to the case with 64^3 modes including the terms. Thus, those terms are not included in the calculations reported here. This reduces the number of Fourier transforms per time step from 45 to 27.

Figure 3 shows how the normalized root-mean-square (rms) velocity develops as a function of time for different frequencies. The nonoscillating case ($\Omega=0$) represents a lower limit for the rms velocity. As the field oscillates at a faster rate, the turbulence intensity increases. The cases with $\Omega\tau_B<1$ are bounded above by the zero-field case ($\xi=0$) at all times in the simulation. Thus, the rms velocity can be bounded above and below by the steady results, provided

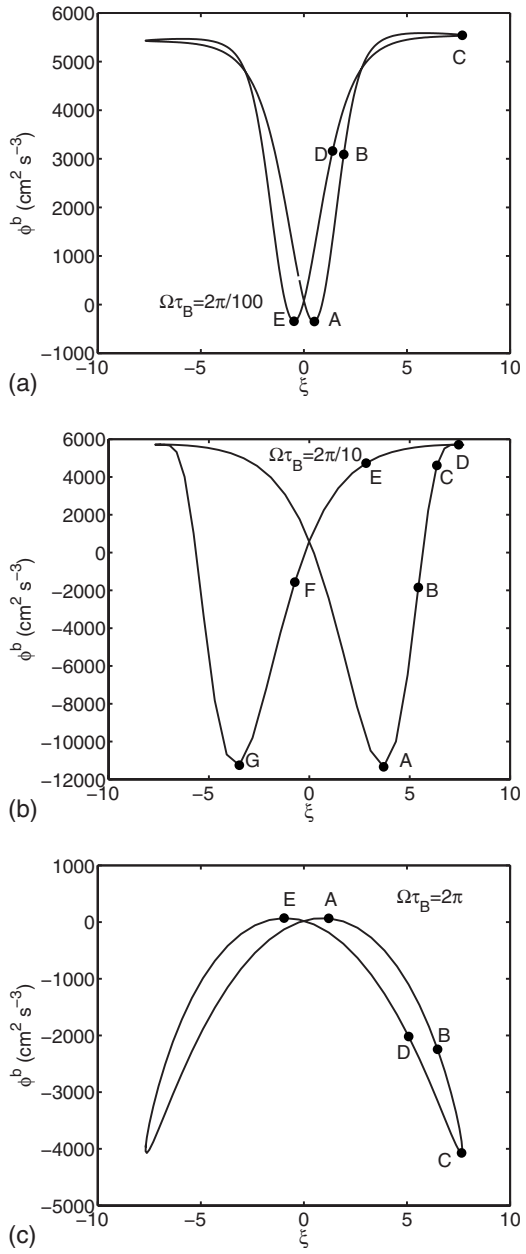

FIG. 8. Limit cycle of transfer rate of kinetic energy to spin energy vs ξ. Magnetic field amplitude of $\xi=7.68$. Oscillation frequencies of (a) $\Omega\tau_B=2\pi/100$, (b) $2\pi/10$, and (c) 2π. The labels (A–E) in panel (a) correspond to Figs. 10(a) and 11(a); labels (A–G) in panel (b) correspond to Figs. 10(b) and 11(b); labels (A–E) in panel (c) correspond to the Figs. 10(c) and 11(c).

$\Omega\tau_B<1$. Schumacher *et al.* [2] showed that the root-mean-squared velocity is decreased as the steady magnetic field is increased; thus the steady results can provide an envelope in which the solution lies for any frequency with $\Omega\tau_B<1$. When $\Omega\tau_B>1$, the turbulent intensity is higher than the zero-field case at all times. This implies that the turbulent flows gain turbulent kinetic energy as $\Omega\tau_B$ increases, at least up to $\Omega\tau_B=2\pi$.

In turbulence, one effect of viscosity is to dampen the fluid motion at large wave numbers. In general, as viscosity decreases, turbulent motion persists to smaller and smaller scales causing the kinetic energy spectrum to broaden and the rms velocity to increase. The effect of applying the oscillating field when $\Omega\tau_B<1$ is similar to an increased effective viscosity in our homogeneous system, and a field with $\Omega\tau_B=2\pi$ is analogous to a decreased effective viscosity. Thus, the concluding observation of Bacri *et al.* [4], that $\mu_{\text{eff}}/\mu<1$ when $\Omega\tau_B\sim1$ for laminar pipe flow is verified numerically to apply to homogeneous turbulence.

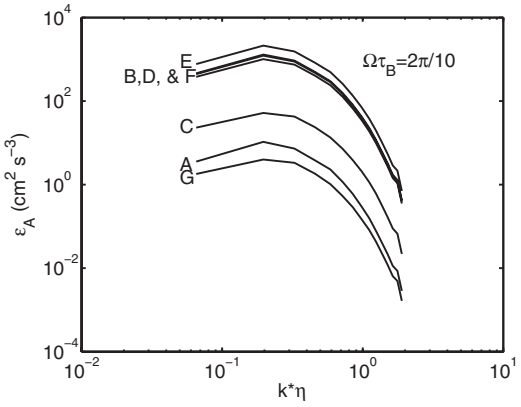

FIG. 9. Vortex viscous dissipation rate spectra vs wavenumber. Magnetic field amplitude of $\xi=7.68$. The labels (A–G) correspond to Fig. 7(b).

Figure 4 shows how the Taylor microscale develops as a function of time. For the cases here, when the $\Omega\tau_B$ gets larger, the Taylor microscale gets smaller. As with the rms velocity, when $\Omega\tau_B<1$ the Taylor microscale is bounded for all times by results for $\xi=7.68$, nonoscillating field, and results for a zero-field case. When $\Omega\tau_B>1$, the Taylor microscale is lower than the zero-field case at all times. This implies that the turbulent length scales decrease as $\Omega\tau_B$ increases, at least up to $\Omega\tau_B=2\pi$.

Next we look at the spin and vorticity behavior over one complete cycle of the magnetic field. The spin is a variable for ferrofluid simulations, and it is directly influenced by both the flow and magnetic field. The spin to vorticity ratio provides information on the net spin-up effect of the particles. Here, we investigate $\langle(2\omega_i')^2\rangle/\langle g_i'^2\rangle$, where $g_i'=\varepsilon_{ikl}u_{l,k}'$ is the vorticity. When this ratio is equal to one, there is no net effect, but when it is greater than one, the particles are on average spinning faster than the surrounding fluid. Note that this ratio is related to the mean square magnetic torque.

First, we observe the spin and vorticity behavior as a function of time over one complete cycle of the applied magnetic field. In Fig. 5, the time behavior of the mean square of twice the spin rate and the mean square vorticity are shown for all three oscillating cases over one complete oscillation cycle of H. The mean squared spin and mean squared vorticity variables are normalized by the mean squared vorticity of the initial velocity field ($t=0$); thus, the normalization factor is the same in all cases. The solid line is the mean squared spin, and the line labeled $\langle g^2\rangle/\langle g_0^2\rangle$ is the mean squared vorticity. The dashed lines represent mean squared spin values with $\xi=0$, $\xi=7.68$, and $\xi=\infty$ for a steady ($\Omega=0$) magnetic field. The time is normalized by the Kolmogorov time of the Newtonian fluid. Figure 5 shows that the

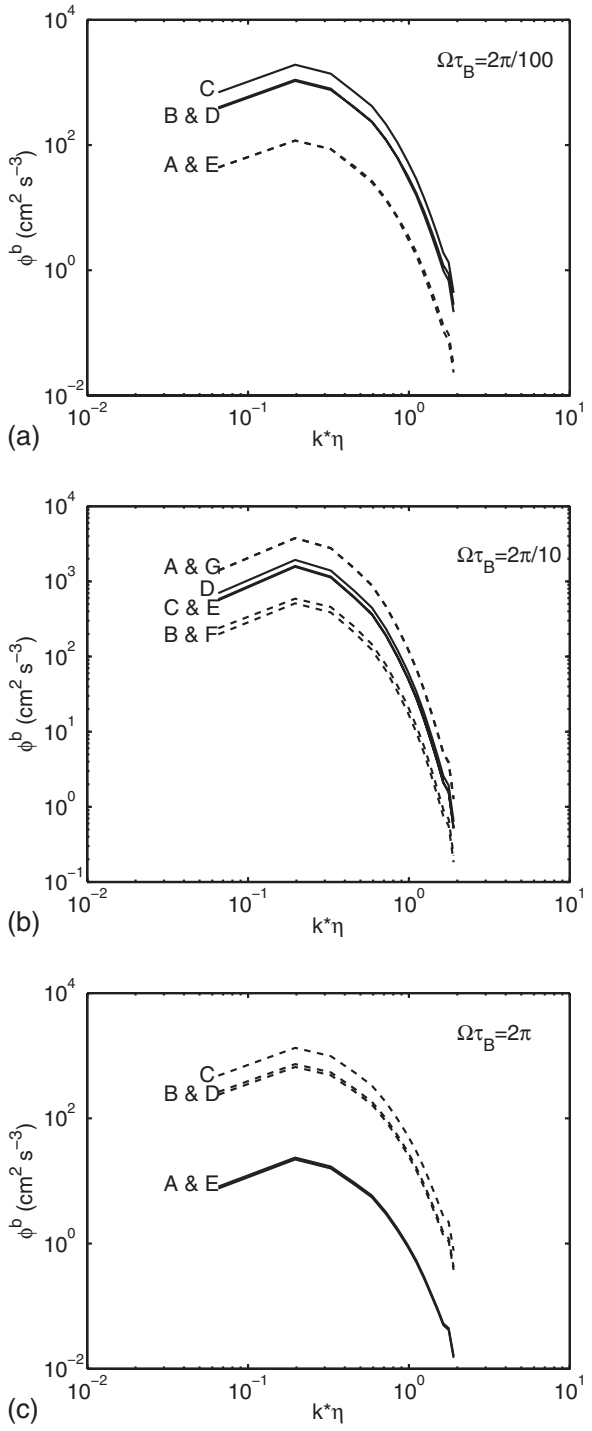

FIG. 10. Spectra plot of the transfer rate of kinetic energy to spin energy vs wavenumber at different times. Magnetic field amplitude of ξ=7.68, and using the Martsenyuk (Ref. [9]) magnetization equation. Oscillation frequencies of (a) $\Omega\tau_B=2\pi/100$, (b) $2\pi/10$, and (c) 2π. The labels (A–E) in panel (a) correspond to Figs. 8(a) and 11(a); labels (A–G) in panel (b) correspond to Figs. 8(b) and 11(b); labels (A–E) in panel (c) correspond to Figs. 8(c) and 11(c).

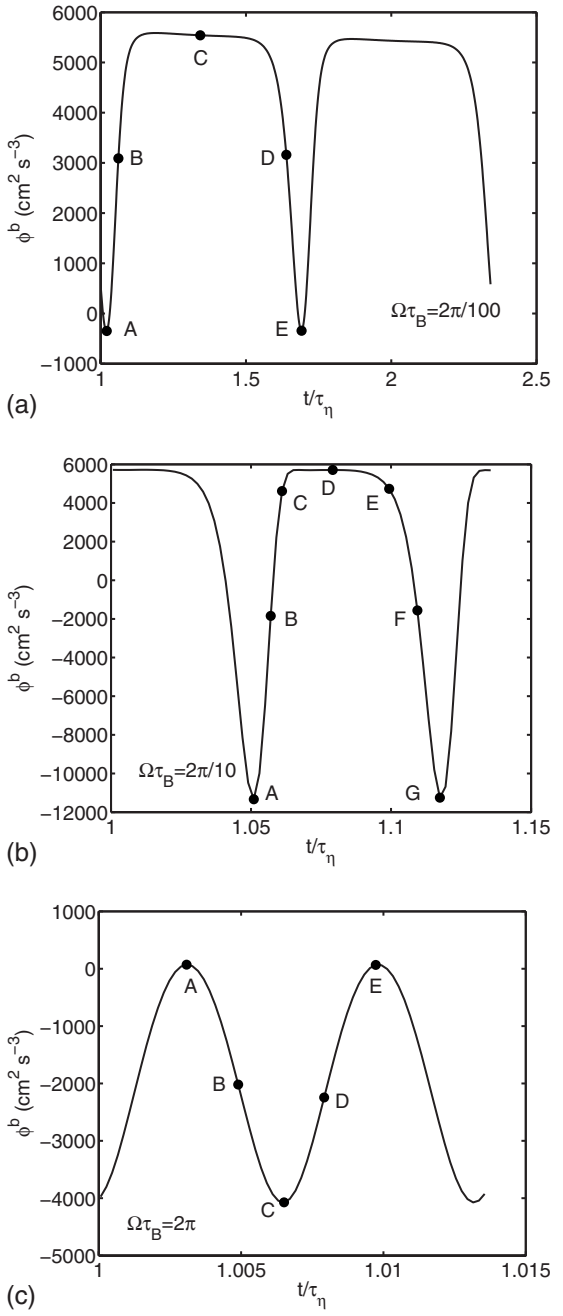

FIG. 11. Transfer rate of kinetic energy to spin energy vs time. Magnetic field amplitude of ξ=7.68, and using the Martsenyuk (Ref. [9]) magnetization equation. Oscillation frequencies of (a) $\Omega\tau_B=2\pi/100$, (b) $2\pi/10$, and (c)2π. The labels (A–E) in panel (a) correspond to Figs. 8(a) and 10(a); labels (A–G) in panel (b correspond to Figs. 8(b) and 10(b); labels (A–E) in panel (c) correspond to Figs. 8(c) and 10(c).

spin exhibits large oscillations while the vorticity is approximately steady. The mean square spin behavior is periodic in time, and completes two cycles every time the magnetic field completes one cycle. Figure 5(a) is at an oscillation frequency of $\Omega\tau_B=2\pi/100$(1 kHz) and the spin has a lower bound determined by the steady case and an approximate upper bound determined by the vorticity. In Fig. 5(b), at $\Omega\tau_B=2\pi/10$(10 kHz), the spin has a lower bound determined by the steady case, but the spin peaks at values about 60% larger than vorticity. At the highest frequency case, $\Omega\tau_B=2\pi$(100 kHz), shown in Fig. 5(c), the spin is above the vorticity the majority of the time; in this case the spin peaks

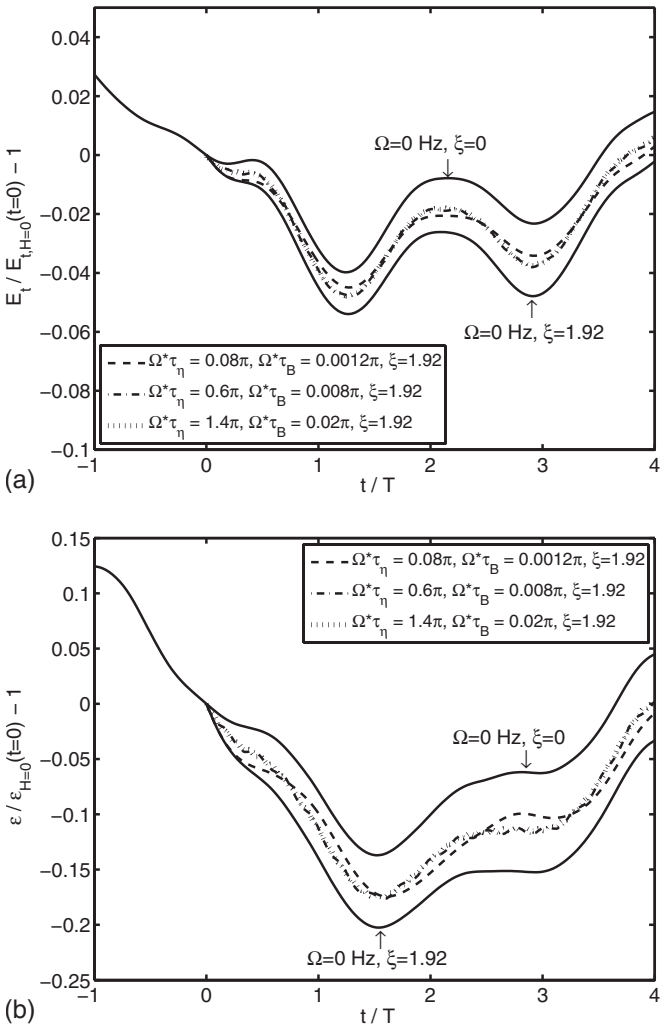

FIG. 12. Fractional turbulent kinetic energy (a), and classical viscous dissipation (b), vs normalized time. The oscillation frequencies (Ω=60, 400, and 1000 Hz) and amplitude (ξ=1.92) correspond with experimental conditions in Schumacher *et al.* (Ref. [6]). The Shliomis (Ref. [8]) magnetization equation is used.

at values about 20% larger than the vorticity and has valleys that are approximately equal to the vorticity. Thus, under these conditions there are substantial differences between twice the spin and the vorticity over a single cycle of **H**.

In Fig. 6, we examine the relationship between the mean square value of twice the spin and the magnitude of the oscillating magnetic field. The mean square value of twice the spin at an instant in time is normalized by the mean square vorticity of the flow at that same instant in time. Each panel of Fig. 6 has labeled dashed lines that represent the ratio for the (ξ=0, Ω=0), (ξ=7.68, Ω=0), and ($\xi\sim\infty$, Ω=0) cases. The large oscillations are approximately periodic and are due to the rapid variations in the particle spin since the vorticity is essentially constant over a period of oscillation. In Fig. 6(a), at $\Omega\tau_B=2\pi/100$(1 kHz) the spin to vorticity ratio is small at high magnetic field strengths. As ξ is decreased toward zero, the spin to vorticity ratio increases toward a value of one. In other words, the spin rate approaches the rotation rate of the fluid as ξ goes to zero. Briefly after the magnetic field changes sign, the spin to vorticity ratio goes above 1,

TABLE III. Time averages of the turbulent kinetic energy and classical viscous dissipation shown in Fig. 12.

Case	$\{E_t\}$ (cm^2 s^{-2})	$\{\varepsilon\}$ (cm^2 s^{-3})
$\Omega=0$, $\xi=0$	634.91	58683
$\Omega=0$, $\xi=1.92$	624.78	54445
$\Omega\tau_B=0.0012\pi$, $\xi=1.92$	629.17	56264
$\Omega\tau_B=0.008\pi$, $\xi=1.92$	629.20	56246
$\Omega\tau_B=0.02\pi$, $\xi=1.92$	629.31	56293

and then promptly begins to decrease toward the ξ=7.68 steady limit. That is, there is a brief moment after the applied oscillating field changes sign where the simulations predict that the particles spin-up and rotate faster than the surrounding fluid. In Fig. 6(b), at $\Omega\tau_B=2\pi/10$, the effect described for Fig. 6(a) is amplified. Once the magnetic field changes sign, the spin-up of the fluid occurs over a larger range of ξ. The spin-up peaks at about ξ=3.5, and then decreases back down toward the ξ=7.68 steady case limit. In Fig. 6(c), at $\Omega\tau_B=2\pi$, the spin ratio is almost always greater than one, and the spin-up peaks when ξ=7.68.

There is a hysteresis effect present in the limit-cycle figures that ensues because of the finite relaxation time of the particle. The spin to vorticity ratio, at a specific ξ, depends on whether the field is increasing or decreasing. The hysteresis disappears as $\Omega\tau_B$ goes to zero, because the particle's magnetization is always coaligned with the applied changing field. The hysteresis also disappears as $\Omega\tau_B$ goes to infinity: no hysteresis is expected to occur because the particle spin cannot rotate fast enough and becomes uncorrelated with the applied field; the line would be the same as the ξ=0 steady limit line.

Shliomis and Morozov [3] (theory), Bacri *et al.* [4] (theory and experiment), and Zeuner *et al.* [5] (experiment) documented the spin-up effect for time averages in laminar pipe flow. We show here for turbulent flow there are brief moments of spin-up that occur even when $\Omega\tau_B<1$, and that they occur routinely at high frequency.

Energy terms that involve velocity only (e.g., the turbulent kinetic energy and classical viscous dissipation rate) do not change significantly during the time it takes the magnetic

TABLE IV. Time averaged flow properties of the initial ferrofluid velocity field.

Flow property	Value
$u_{\rm rms}$ (cm s^{-1})	2.5
$\mathcal{L}$ (cm)	1.2
$\mathcal{T}$ (s)	0.474
Re_λ	49.0
λ (cm)	0.64
η (cm)	0.046
τ_η (s)	0.0625
$k_{\rm max}\eta$	1.5

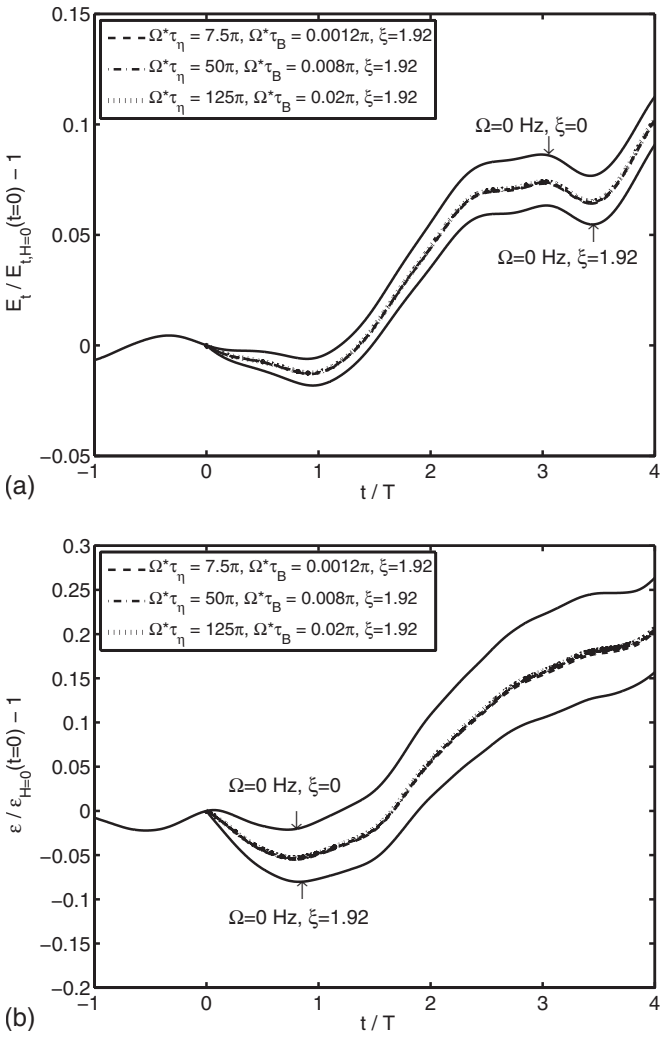

FIG. 13. (a) Fractional turbulent kinetic energy, and (b) classical viscous dissipation rate vs normalized time. Similar magnetic field conditions as Fig. 12, but for flow conditions described in Table IV. The Shliomis (Ref. [8]) magnetization equation is used.

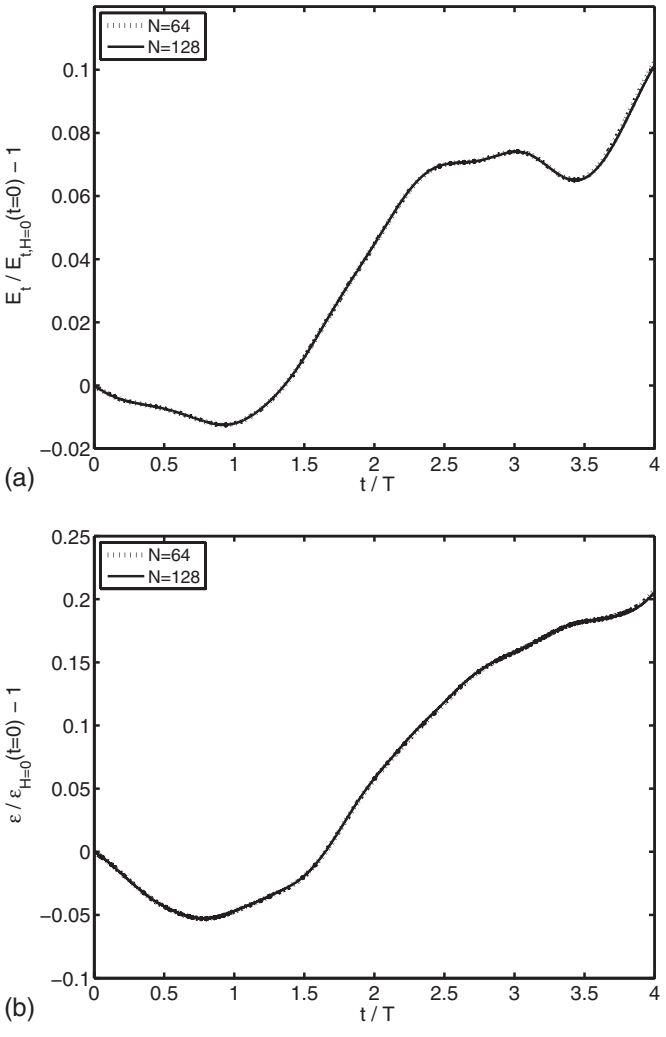

FIG. 14. Fractional turbulent kinetic energy (a), and classical viscous dissipation rate (b), vs normalized time. The simulation using 64^3 Fourier modes is superimposed on the results obtained when using 128^3 modes. Same conditions as the 1000 Hz case in Fig. 13. The Shliomis (Ref. [8]) magnetization equation is used.

field to complete one cycle. However, the energy terms that involve the spin, e.g., ε_A, Φ^b, and ψ_s, exhibit pronounced periodic behavior and complete two cycles every time **H** completes one. Next, we investigate the limit-cycle behavior of ε_A and Φ^b. (Note that $\Phi^b = -\psi_s$ since the spin viscous dissipation and moment of inertia terms are negligible.) Figures 7 and 8 show the limit cycles of ε_A and Φ^b, respectively. Note that although ε_A is always greater than zero, the Φ^b exhibits both positive and negative values. As shown in Fig. 7, for each case, ε_A reaches a maximum value when the magnetic field is strongest, and there is a visual hysteresis in the limit-cycle plots. The value of vortex viscous dissipation depends on the magnitude of **H** and how it changes in time. This hysteresis effect is due to the finite relaxation time of the ferrofluid particles. In Fig. 7(b), after the magnetic field changes sign, there is a hump in the limit cycle. This occurs because of the particle spin-up. The parameter Φ^b represents the transfer rate of kinetic energy to spin energy, and this is plotted in Fig. 8. The Φ^b ranges from mostly positive values in Fig. 8(a), to a range of positive and negative values in Fig. 8(b), to mostly negative values in Fig. 8(c). When Φ^b is positive, the particles are rotating slower than the surrounding fluid, and translational kinetic energy is being converted into rotational kinetic energy. When negative, the particles are rotating faster than the surrounding fluid, and rotational kinetic energy is being converted into translational kinetic energy. In Figs. 8(a) and 8(b), when the magnetic field changes sign and rotates the particles faster than the surrounding fluid, the Φ^b drops down into negative values. In Fig. 8(c), Φ^b appears to always be negative, meaning that spin energy is constantly being converted into kinetic energy of the flow. Thus, when Φ^b is negative, it acts as a forcing term and leads to a more intense turbulent flow as well as an additional energy dissipation. In an oscillating field, energy can flow back and forth between translational and spin kinetic energy.

Next, we consider the spectral wave number distribution of the $\varepsilon_A(k)$ and $\phi^b(k)$ energy terms at various instances over the period of oscillation. Figure 9 illustrates the $\varepsilon_A(k)$ spectra for the $2\pi/10$ case. The three panels of Fig. 10 shows the

$\phi^b(k)$ spectra for the $2\pi/100$, $2\pi/10$, and 2π cases. Again, ϕ^b is not strictly positive, and becomes negative over a portion of the oscillation cycle. Therefore, since $\phi^b(k)$ is plotted on a logarithmic scale in Fig. 10, the solid lines denote where $\phi^b(k)$ is positive and dashed lines represent $|\phi^b(k)|$ when it is less than zero. At the different instances over the period of oscillation, the general shapes of the $\varepsilon_A(k)$ and $\phi^b(k)$ spectra do not change significantly, rather the entire spectrum is just shifted up or down depending on the magnitude of **H** at the specific time.

In Fig. 11, Φ^b is plotted vs time. The Φ^b ranges from mostly positive values in Fig. 11(a), to a range of positive and negative values in Fig. 11(b), to mostly negative values in Fig. 11(c).

C. Homogeneous simulations at experimental conditions

In this section, we examine the homogeneous simulations at magnetic field amplitude 316 Oe ($\xi=1.92$) and oscillation frequencies of 60, 400, and 1000 Hz. These values correspond to some of the experimental conditions of the turbulent pipe flow experiment of Schumacher *et al.* [6]. In the experiment, when the flow was turbulent, changing the oscillation frequency in the 60–1000 Hz range at amplitude $\xi=1.92$ had a minimal effect on the measured pressure drop. Our goal is to examine if our homogeneous simulation results correspond to these experimental conditions of the turbulent pipe flow experiment of Schumacher *et al.* [6]. For all cases in this section, the Shliomis [8] magnetization equation is employed.

Figure 12 shows the time development of turbulent kinetic energy (E_t) and classical viscous dissipation (ε) for each frequency. The results of the nonoscillating case ($\xi=1.92$, $\Omega=0$) and the no magnetic field case ($\xi=0$) are also shown. The lines at different Ω values are not superimposed, but are bounded by the ($\xi=0$) case and ($\xi=1.92$, $\Omega=0$) case. Time-averaged values (denoted by $\{\cdot\}$) of E_t and ε are given in Table III and, for the cases at 60, 400, and 1000 Hz, the $\{E_t\}$ and $\{\varepsilon\}$ are effectively independent of the frequency of oscillation. Thus, changing the oscillation frequency within the experimental range had minimal effect on the time-averaged turbulence properties. This corresponds well with the experimental observation of Schumacher *et al.* [6].

D. Effect of increasing turbulence scales

We are also interested in comparing the results of Fig. 12 to the turbulence behavior in cases where the magnetic field oscillates much faster than the Kolmogorov time, i.e., $\Omega\tau_\eta \gg 1$. The homogeneous turbulent flow is adjusted such that the turbulent time scales are large relative to the period of oscillation of the magnetic field. The properties of the initial velocity field are listed in Table IV, where, for example, the Kolmogorov time is now $\tau_\eta=0.0625$ s. The same magnetic field and ferrofluid parameters used to produce Fig. 11 are used here: the oscillation frequencies are 60, 400, and 1000 Hz, and the particle relaxation time is 10^{-6} s. Thus, $\Omega\tau_\eta$ changes for these cases, but $\Omega\tau_B$ stays the same. In Fig. 13, the oscillating cases all differ from the base case and steady case, but do not differ from each other significantly. The overall influence of the field on the turbulent kinetic energy and classical viscous dissipation is almost independent of increasing the oscillation frequency. Thus, making the magnetic field oscillate at 60 Hz has an effect on the turbulence, but the effect is unchanged with frequencies up to 1000 Hz. All the simulations shown in Fig. 13 are done with 64^3 modes, but the difference between the solution with 64^3 modes and 128^3 modes is small (Fig. 14).

IV. CONCLUSIONS

This paper examines the effects of an axially oscillating magnetic field on homogeneous ferrofluid turbulence. When $\xi=1.92$ and $\Omega\tau_B=0.02\pi$, the flow results are essentially independent of magnetic equation, and this result can probably be generalized for all results where $\xi<2$ and $\Omega\tau_B\leq 0.02\pi$.

When $\Omega\tau_B=2\pi$, the particles spin faster than the surrounding fluid, and energy is injected into the system. In slow laminar pipe flows this result has been observed experimentally [4,5] in terms of a reduced effective viscosity. These laminar flows of course had a nonzero mean shear rate, and it is shown here that this phenomenon is possible for turbulent flows with a zero mean shear as well. The average vorticity of our system is zero, so the effect must be due to the fluctuating part of the rotational motion of this particular turbulent flow. From the results of Φ^b at the highest frequency, energy is continually transferred from rotational kinetic energy to translational kinetic energy. For the lower frequency magnetic fields examined, energy was continually flowing back and forth between translational and rotational modes.

In the cases where the magnetic field conditions corresponded to the turbulent pipe flow experiments [6], the time-averaged results are almost independent of oscillation frequency. This is consistent with the experimental results that show an independence of fractional pressure drop on frequency. Finally, we note that, at all times in our simulations, the turbulent results for an oscillating magnetic field are bounded between curves for a Newtonian fluid and a ferrofluid with a large, steady magnetic field.

ACKNOWLEDGMENT

This work was supported by NSF under Grant No. CTS-347044.

[1] J. McTague, J. Chem. Phys. **51**, 133 (1969).
[2] K. R. Schumacher, J. J. Riley, and B. A. Finlayson, J. Fluid Mech. **599**, 1 (2008).
[3] M. I. Shliomis and K. I. Morozov, Phys. Fluids **6**, 2855 (1994).
[4] J. C. Bacri, R. Perzynski, M. I. Shliomis, and G. I. Burde, Phys. Rev. Lett. **75**, 2128 (1995).
[5] A. Zeuner, R. Richter, and I. Rehberg, Phys. Rev. E **58**, 6287 (1998).
[6] K. R. Schumacher, I. Sellien, G. S. Knoke, T. Cadar, and B. A. Finlayson, Phys. Rev. E **67**, 026308 (2003).
[7] R. E. Rosensweig, *Ferrohydrodynamics* (Cambridge University Press, Cambridge, New York, 1985).
[8] M. I. Shliomis, Zh. Eksp. Teor. Fiz. **61**, 27411 (1972) [Sov. Phys. JETP **34**, 1291 (1972)].
[9] M. A. Martsenyuk, Y. L. Raikher, and M. I. Shliomis, Sov. Phys. JETP **38**, 413 (1974).
[10] B. U. Felderhof and H. J. Kroh, J. Chem. Phys. **110**, 7403 (1999).
[11] O. Zikanov and A. Thess, J. Fluid Mech. **358**, 299 (1998).
[12] S. B. Pope, *Turbulent Flows* (Cambridge University Press, Cambridge, UK, 2000).
[13] R. Kerr, J. Fluid Mech. **153**, 31 (1985).
[14] T. Gotoh, D. Fukayama, and T. Nakano, Phys. Fluids **14**, 1065 (2002).
[15] Y. Kaneda, T. Ishihara, M. Yokokawa, K. Itakura, and A. Uno, Phys. Fluids **15**, L21 (2003).